J Solid State Electrochem (2008) 12:445–451
DOI 10.1007/s10008-007-0405-2

ORIGINAL PAPER

Modeling of solvent viscosity effects on the electroreduction of Pt(II) aquachlorocomplexes

Renat R. Nazmutdinov · Michael D. Bronshtein · Dmitrii V. Glukhov · Tamara T. Zinkicheva

Received: 6 March 2007 / Revised: 14 May 2007 / Accepted: 4 June 2007 / Published online: 21 September 2007

Abstract Solvent dynamics effects on the electroreduction of $[PtCl_3(H_2O)]^-$ at a mercury electrode are explored in the framework of Sumi–Marcus model using an efficient computational scheme. According to results of density functional calculations, the second electron transfer step may be regarded as rate controlling. The nonmonotonous influence of solvent viscosity on the reaction rate is predicted and explained in terms of the saddle point avoidance. The results of model calculations are employed to interpret experimental data reported earlier in the literature.

Keywords Electron transfer · Solvent dynamics · Sumi–Marcus model · Density functional calculations · Pt(II) aquachlorocomplexes

Introduction

The interplay between solvent dynamics (viscosity effects) and intramolecular reorganization in adiabatic electron transfer (ET) reactions can be addressed in the framework of the Sumi–Marcus (SM) model [1, 2]. Various applications of this model (frequently referred to the Agmon–Hopfield formalism in literature) were intensively investigated over the last two decades [3–19]. However, despite considerable progress in this field, some problems are not properly understood so far. Chemical reactions proceeding in solution bulk were presumed in most studies, while only a few attempts were made to explore electrochemical ET processes [17–19]. The heterogeneous ET kinetics was never studied in terms of the SM model for a wide interval of the reaction-free energy. In part, although certain activationless homogeneous processes were examined in terms of the Agmon–Hopfield formalism [20, 21], this method was not employed to model electrode reactions in activationless kinetic regime. Comparison with electrochemical experiments also remains an apparent bottleneck for relevant calculations. Ample experimental material on the viscosity effects thoroughly reviewed in Fawcett and Foss [22], Weaver [23], and Fawcett and Opallo [24] relates to certain electrode processes taking place in a narrow overpotential region without noticeable intramolecular reorganization. That is why exploiting the SM model to describe interfacial ET reactions may be regarded as a hot area of research. A set of parameters that crucially affect the results of model calculations can be obtained using a quantum chemical approach.

In this work, we consider electrochemical reduction of Pt(II) aquachlorocomplexes from aqueous solutions at a mercury electrode. This two-step reaction was studied experimentally for a long time using classical electrochemical methods [25–31]. The reaction proceeds at high electrode overpotentials (in the vicinity of activationless discharge) and reveals a remarkable feature-pit on the polarization curves. Recently, the solvent dynamics effects on the electroreduction of Pt(II) aquachlorocomplexes were addressed for the first time using polarographic technique [31] (sucrose was employed as a viscosity-forming additive). The authors [31] estimated the "adiabaticity degree" (θ), a quantity that can be treated as a measure of the influence of solvent dynamics on the reaction rate. The dependence of θ as a function of the electrode overpotential was found to be non-

Dedicated to Professor Oleg Petrii on the occasion of his 70th birthday on August 24th, 2007

R. R. Nazmutdinov (✉) · M. D. Bronshtein · D. V. Glukhov · T. T. Zinkicheva
Kazan State Technological University,
K. Marx Str., 68,
420015 Kazan, Republic Tatarstan, Russian Federation
e-mail: nazmutdi@kstu.ru

monotonous passing a maximum. This challenging effect is of a qualitative nature and calls for theoretical explanation.

We report below the results of modeling of the solvent dynamics effects on the mechanism of electroreduction of Pt(II) aquachlorocomplexes at a mercury electrode combining the SM model and quantum chemical calculations. A novel point is an extension of the SM model to region of high overpotentials. Because it was shown in Nazmutdinov et al. [32] (in preparation) that a $[PtCl_3(H_2O)]^-$ complex (the product of hydrolysis of $[PtCl_4]^{2-}$) is the most probable electrochemically active form, we restrict ourselves to considering this reactant solely. The paper is organized as follows: The pertinent details of model calculations are reported in "Model and computational details". The computational results are discussed and compared with experimental data in the section "Results and discussion". Some concluding remarks can be found in the last section, "Concluding remarks."

It is our pleasure to dedicate this work to our colleague Prof. Oleg A. Petrii, who contributed significantly to experimental studies of the electrochemical reduction of various anions.

Model and computational details

Dealing with the SM model we have to solve the Smoluchowski equation complemented by a sink term,

$$\frac{dP(q,\tau)}{d\tau} = D\frac{\partial}{\partial q}\left\{\frac{\partial}{\partial q} + \frac{1}{kT}\frac{d}{dq}U(q)\right\}P(q,\tau) - k_{\text{in}}(q)P(q,\tau), \quad (1)$$

where q is the dimensionless solvent coordinate; $P(q, \tau)$ is the probability density to find a reactant in initial state; D refers to the diffusion coefficient, $D = \frac{kT}{2\lambda_s\tau_L}$; λ_s is the solvent reorganization energy; τ_L is the effective solvent relaxation time (for non-Debye solvents, this quantity is discussed in Nazmutdinov et al. [19]); and $U(q)$ is a section of the reaction free energy surface (RFES).

Although adiabatic ET is assumed, it is convenient to construct two diabatic RFES describing the well-known symmetric Marcus barrier for one-ET [33]:

$$U_i(q, q_{\text{in}}) = \lambda_s q^2 + \lambda_{\text{in}} q_{\text{in}}^2 \quad (2)$$

and

$$U_f(q, q_{\text{in}}) = \lambda_s(q-1)^2 + \lambda_{\text{in}}(q_{\text{in}}-1)^2 + W_f - W_i - F\eta,$$

where indices i and f refer to the initial (i) and final (f) reaction states, respectively; q_{in} is the dimensionless intramolecular coordinate; λ_{in} is the energy of intramolecular reorganization; η is the electrode overpotential; and W_i and W_f are the work terms of reactant and product.

The effect of the orbital overlap on the RFES shape was neglected; the latter can be addressed in terms of the Anderson Hamiltonian [34]. The sink term in Eq. 1, $k_{\text{in}}(q)$, is written as follows:

$$k_{\text{in}} = \nu_{\text{in}} \exp\left\{-\Delta E_a^*(q)/kT\right\}, \quad (3)$$

where ν_{in} is an effective frequency factor (10^{-13} c^{-1}), which characterizes the intramolecular reorganization.

The energy barrier along the intramolecular degree of freedom coordinate, ΔE_a^*, depends on the solvent coordinate q and is defined in the form

$$\Delta E_a^*(q) = U\left(q, q_{\text{saddle}}^*(q)\right) - U(q, q_{\text{in}} = 0) = U\left(q, q_{\text{saddle}}^*(q)\right) - U(q), \quad (4)$$

where q_{saddle}^* (q) notes the RFES saddle line. Tunnel effects which may facilitate overcoming the energy barrier along q_{in} were neglected.

The probability density $P(q,\tau)$ is described by the initial-boundary problem

$$P(q,\tau)\Big|_{\tau=0} = P_0(q) = \frac{1}{N}\exp\left(-\lambda_s q^2/kT\right), \quad (5)$$

and

$$\frac{\partial P(q,\tau)}{\partial q} + \frac{1}{kT}\frac{\partial U(q)}{\partial q}P(q,\tau)|_{q=a} = 0,$$

where N is the normalization coefficient ($N = \sqrt{\lambda_s/\pi kT}$); a=q_L or q_R (q_L and q_R are assumed q values at the left and right boundaries, respectively).

Then the ET rate constant (k_s) can be defined as follows:

$$1/k_s \approx \int_0^\infty d\tau \int_{q_L}^{q_R} P(q,\tau)dq. \quad (6)$$

Another definition of k_s is discussed in Sumi and Marcus [1] and Nadler and Marcus [2]. For heterogeneous ET, k_s should be multiplied by the reaction volume to be compared with experiment. Analytical solutions of Eq. 1 for some special limiting cases were reported earlier (see, e.g., [1–3, 5, 10]). However, effective numerical schemes that provide stable solutions for a wide range of both the reaction free energy and solvent viscosity are still lacking. We describe below in brief a new computational approach to handle this problem.

It is convenient to introduce a new function $y(q)$:

$$y(q) = P^*(q)\exp\{U(q)/kT\}, \quad (7)$$

where $P^*(q) = \int_0^\infty P(q,\tau)d\tau$.

It is evident that the rate constant can be recast as

$$1/k_s = \int_{q_L}^{q_R} y(q) \exp\{-U(q)/kT\} dq, \tag{8}$$

In turns, for $y(q)$ we have the following boundary value problem:

$$\frac{d^2y(q)}{dq^2} - \frac{1}{kT}\frac{\partial U(q)}{\partial q}\frac{dy(q)}{dq} - (k_{in}/D)y(q) = -(P_0(q)/D)\exp\{U(q)/kT\}. \tag{9}$$

Using the classical Cauchy method of variation of constants, the solution of this problem can be constructed in the form:

$$y(q) = \frac{1}{D}\int_{q_L}^{q} \frac{\exp\{\varphi_R(q) - \varphi_R(\xi) + U(q)/kT\}}{\psi_L(\xi) - \psi_R(\xi)} P_0(\xi) d\xi + \frac{1}{D}\int_{q}^{q_R} \frac{\exp\{\varphi_L(q) - \varphi_L(\xi) + U(q)/kT\}}{\psi_L(\xi) - \psi_R(\xi)} P_0(\xi) d\xi, \tag{10}$$

where $\varphi_L(q)$ and $\varphi_R(q)$ are antiderivatives to $\psi_L(q)$ and $\psi_L(q)$, respectively, i.e., $\varphi_L(q) = \int_{q_L}^{q} \psi(\xi) d\xi$ and $\varphi_R(q) = \int_{q}^{q_R} \psi(\xi) d\xi$.

The functions ψ_L and ψ_R in Eq. 10 are solutions of the differential equation:

$$\frac{d\psi(q)}{dq} + \psi^2 - \frac{1}{kT}\frac{\partial U(q)}{\partial q}\psi = k_{in}(q)/D, \tag{11}$$

which is solved numerically for two different boundary conditions: $\psi_L(q_L) = 0$ and $\psi_R(q_R) = 0$.

If $\int_{q_L}^{q_R} k_{in}(q) dq/D << 1$ (region of small viscosity values), then both ψ_L and ψ_R are close to zero, and the solution of Eq. 9 might be unstable. In this case, a more reliable method is

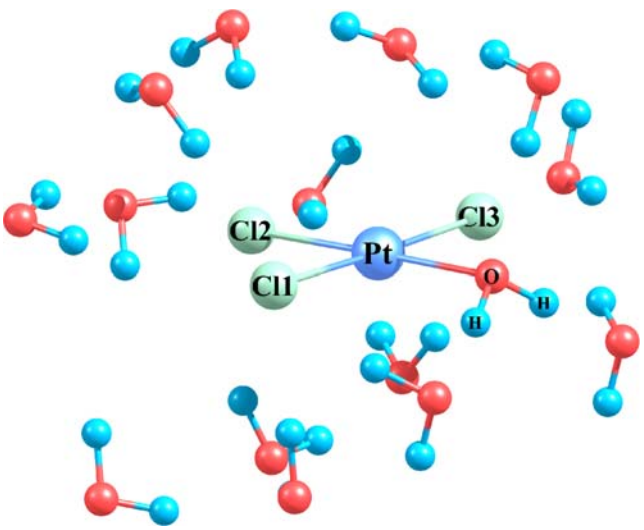

Fig. 1 Optimized stick–ball structure of $[PtCl_3(H_2O)]^{2-}\cdot 10H_2O$

Table 1 Selected bond lengths (nm) and valence angles (grad) obtained from the DFT calculations for the $[PtCl_3(H2O)]^z$ ($z=-1, -2$) complex surrounded with n water molecules ($n=10, 14$)

	$[PtCl_3(H2O)]^-\cdot 10H_2O$ ox. state[a]	$[PtCl_3(H2O)]^{2-}\cdot 10H_2O$ red. state
r(Pt–Cl_1)	0.2387 (0.2387)[b]	0.2665
r(Pt–Cl_2)	0.2346 (0.2347)	0.2496
r(Pt–Cl_3)	0.24 (0.2408)	0.2642
r(Pt–O[c])	0.2138 (0.2117)	0.2389
∠ (Cl_1–Pt–Cl_2)	90 (88.5)	95.1
∠ (Cl_2–Pt–Cl_3)	90.5 (90.1)	93.1
∠ (Cl_1–Pt–O)	89.9 (91.1)	85.8
∠ (Cl_3–Pt–O)	89.6 (90.3)	86.5

[a] r(Pt–Cl)=0.2304 nm obtained for $K_2[PtCl_4]$ in aqueous solution by extended X-ray absorption fine structure spectroscopy) [41]
[b] The results obtained for $[PtCl_3(H_2O)]^-\cdot 14H_2O$
[c] Water molecule from the nearest coordination shell

expanding $P(q, \tau)$ in the eigenfunctions $f_n(q)$ of operator $\widehat{L}^*\widehat{L} + k_{in}$:

$$P(q,\tau) = \sum_{n=0}^{\infty} c_n \exp\{-\lambda_n \tau\} f_n(q), \tag{12}$$

where operator $\widehat{L}$ is defined in the form:

$$\widehat{L} = \exp\{-U(q)/kT\}\frac{\partial}{\partial q}\exp\{U(q)/kT\} \tag{13}$$

and the conjugated operator $\widehat{L}^*$ is written as $\widehat{L}^* = -\frac{\partial}{\partial q}$.

It is easy to solve equation $\left(\widehat{L}^*\widehat{L} + k_{in}\right)f_n = \lambda_n f_n$ numerically. Then the coefficients c_n in expansion 12 are found using the formula:

$$c_n = \frac{\int_{q_L}^{q_R} f_0(q) f_n(q) dq}{\int_{q_L}^{q_R} f_n^2(q) dq}. \tag{14}$$

Several first members in series 12 already yield solution with sufficient accuracy for the region of small viscosity values (usually in this case $n \leq 1$). In contrast, when the solution viscosity is large, this method is no longer effective because the kinetic regime of the reaction becomes strongly multiexponential and we have to deal with a large number of series members.

An efficient estimate of the rate constant in the region of large overpotential values (i.e., in the vicinity of activation-less discharge) is suggested as well:

$$1/k_s \approx 1/v_{in} + \int_{q_L}^{q_B} \{1 - (k_{in}(\xi)/v_{in})\} P^*(\xi) d\xi, \tag{15}$$

where q_B is the crossing point of saddle line and the solvent coordinate (at $q_{in}=0$).

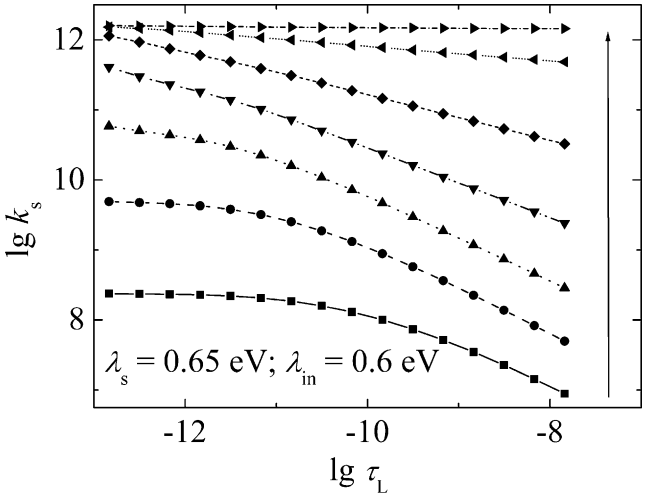

Fig. 2 The lgk_s vs lgτ_L dependencies modeling the first ET in the $[PtCl_3(H_2O)]^-$ reduction calculated for different overpotentials (η). The increasing of η values from 0.2 to 1.2 V is shown by the *arrow*

All simulations were performed assuming the room temperature (T=300 K). The quantum chemical calculations were done at the Density Functional Theory level; the B3LYP hybrid functional was employed as implemented in the Gaussian 03 program suite [35]. To address the solvent effects, 14 or 10 water molecules were included in the coordination shell of $[PtCl_3(H_2O)]^z$ (z=−1, −2, −3), see Fig. 1.

The geometry of the complex reactant in oxidized and reduced states was fully optimized without any symmetry constraints. The open shell system was treated on the basis of spin-polarized (unrestricted) version of the Kohn–Sham equations. The electrons of the Cl, O and H atoms were described by using the 6-311++G(d, p) standard basis set of triple-Z quality [35]. The valency 5*d* 6*s* 6*p* electronic shell of the Pt atom was treated in terms of a basis set of DZ quality [36]; the relativistic core potential developed by Hay and Wadt (LanL2) [35, 36] was employed to describe the effect of inner electrons.

Table 2 Coordinates of the reaction window ($\widetilde{q}$, $\widetilde{q}_{in}$) calculated at several lgτ_L and overpotential values (λ_s=0.65 eV, λ_{in}=0.6 eV)

-lgτ_L	12.2[a]		10.8		9.5	
η/V	0.2	0.6	0.2	0.6	0.2	0.6
$\widetilde{q}$	0.42	0.24	0.4	0.18	0.35	0.1
$\widetilde{q}_{in}$	0.42	0.27	0.44	0.34	0.5	0.44

[a] for this τ_L value a deviation of $\widetilde{q}$ and $\widetilde{q}_{in}$ from the saddle point is negligibly small

Results and discussion

According to the density functional calculations the first ET results in a noticeable lengthening of the Pt–Cl and Pt–O bonds, while the change of the valency angles is rather small (Table 1); the bond break is not observed. The intramolecular reorganization energy was estimated to be 0.6 eV (the small asymmetry of reorganization was neglected). Using the Polarized Continuum Model as implemented in the Gaussian 03 package with a value of 78 for the dielectric constant of water we have computed the solvation free energy of $[PtCl_3(H_2O)]^-$ (−2.08 eV) and appraised its effective radius (0.34 nm, see some pertinent details in Nazmutdinov et al. [37]). The model developed by Kharkats et al. [38] was employed to compute the solvent reorganization energy (λ_s=0.52÷0.65 eV in the interval 0.4÷0.65 nm for the electrode–Pt distance). A value of 5 was taken for the dielectric constant of the interlayer and a factor of 0.8 was used to address the effect of quantum modes on the solvent reorganization. The results of model calculations are practically not sensitive to changing the interlayer thickness from 0.4 to 0.6 nm.

In contrast, the transfer of second electron entails an exceedingly strong reorganization of the $[PtCl_3(H_2O)]^-$ coordination shell with the break of the Pt–O and Pt–Cl_{trans} bonds. The model dissociative process ($[PtCl_3(H_2O)]^{3-}$=Pt^0+$3Cl^-$+H_2O) in aqueous solution was estimated to be feasible as well (the geometry of complex was fixed as obtained for

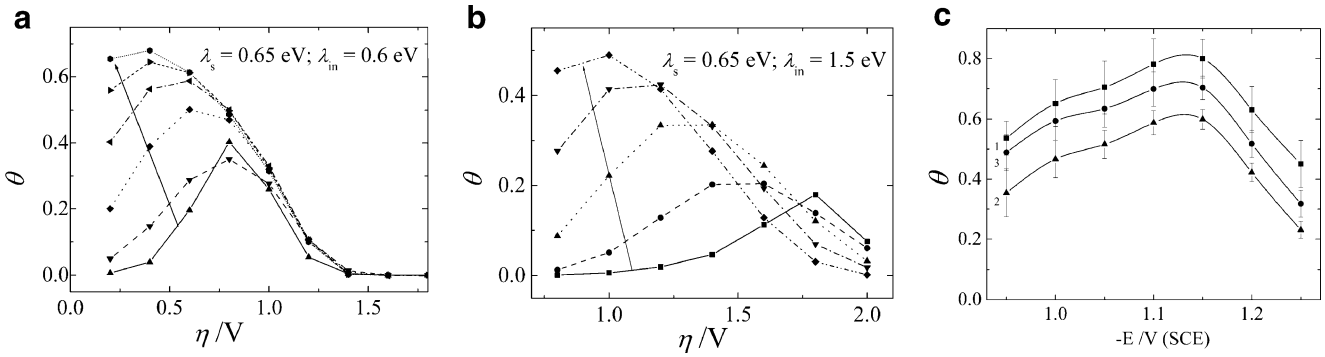

Fig. 3 Model $\theta(\eta)$ dependencies computed for two different λ_{in} values, 0.6 eV (**a**) and 1.5 eV (**b**); the increasing of lgτ_L values from −12.8 to −7.8 is indicated by the *arrow*. **c** Experimental θ vs mercury electrode potential (E) dependencies taken from Pobelov et al. [31]. The curves shown in **c** correspond to three different ways to address the sucrose adsorption; an assumed region of lgτ_L values covers ca two orders (−12<lgτ_L<−10)

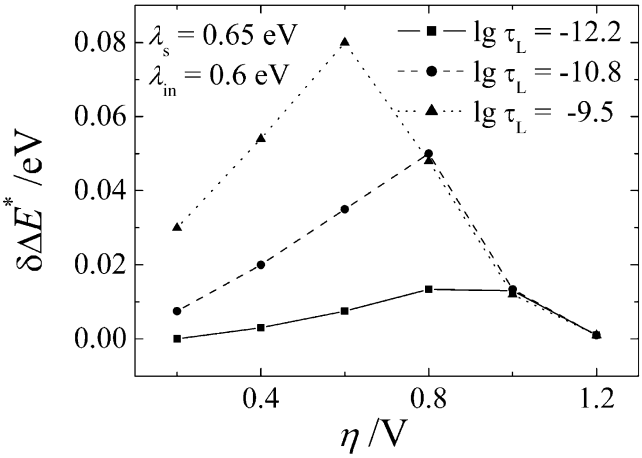

Fig. 4 Model $\delta\Delta E_a^*$ vs η dependencies (see Eq. 16) calculated for three different $\lg\tau_L$ values

the reduced form of $[PtCl_3(H_2O)]^-$). Therefore, the second ET step should be definitely regarded as rate controlling for the reaction under study. A real free energy surface describing this reaction step is multidimensional and anharmonic; its construction is out of the scope of this paper, being a very complicated computational problem. That is why we performed calculations based on the SM model for two different values of intramolecular reorganization energy: the first one, 0.6 eV, relates to the first ET step (see above), while an assumed large value of 1.5 eV roughly characterizes the next step. Such a simplified approach enables, nevertheless, to predict main qualitative tendencies. As two contributions to the total reorganization energy (λ_s and λ_{in}) completely define the shape of free energy surface given by Eq. 2, one can start with further simulations. Note that the W_f–W_i term in Eq. 2 is not easy to estimate (Nazmutdinov et al., in preparation). As this contribution leads, however, only to a simple renormalization of overpotential scale, it was neglected in our calculations.

The $\lg k_s$ vs $\lg\tau_L$ dependencies calculated at several overpotentials and λ_{in}=0.6 eV are shown in Fig. 2. It can be seen that the $\lg k_s$ values become noticeably lower at increasing $\lg\tau_s$. This effect disappears with the growth of η; in the vicinity of activationless discharge the rate constant practically does not depend on the viscosity. The behavior of ϑ vs η $\left(\vartheta = -\frac{d\lg k_s}{d\lg\tau_L}\right)$ in a certain range of the solvent viscosity is displayed in Fig. 3a. As can be seen from this figure, the model curves pass a maximum, which is shifted to smaller ovepotentials when decreasing the τ_L values. Calculations performed for a larger λ_{in} value (1.5 eV) demonstrate qualitatively very similar results (Fig. 3b). At the same time, increasing the intramolecular reorganization predicts smaller ϑ values, which are noticeably shifted to larger overpotentials.

Our results agree, at least qualitatively, with the experimental data reported in Pobelov et al. [31] (see Fig. 3c). As the standard electrode potential of the reaction $[PtCl_4]^-$+ $2e=Pt^{2+}+Cl^-$ is known to be +0.75 V (NHE), the maximum of experimental $\vartheta(\eta)$ dependencies relates to a value of ca 1.7 V in the overpotential scale. Thus, the position of humps on the curves presented in Fig. 3b (which might be ascribed to the second ET step) is closer to that observed in the experiment. On the other hand, the computational data modeling the first reduction step (Fig. 3a) demonstrate the ϑ values, which are in better agreement with the experimental data. We can also maintain that very small values of ϑ in the right region of overpotentials (with respect to the $\vartheta(\eta)$ maximum) give an additional evidence of the activationless nature of the reaction.

The reason of strongly nonmonotonous behavior of $\vartheta(\eta)$ (i.e., the conspicuous influence of solvent viscosity on the ET rate) may be explained in terms of the saddle point avoidance. The origin of this interesting effect resides in the diffusive character of slow solvent coordinate q. Let us

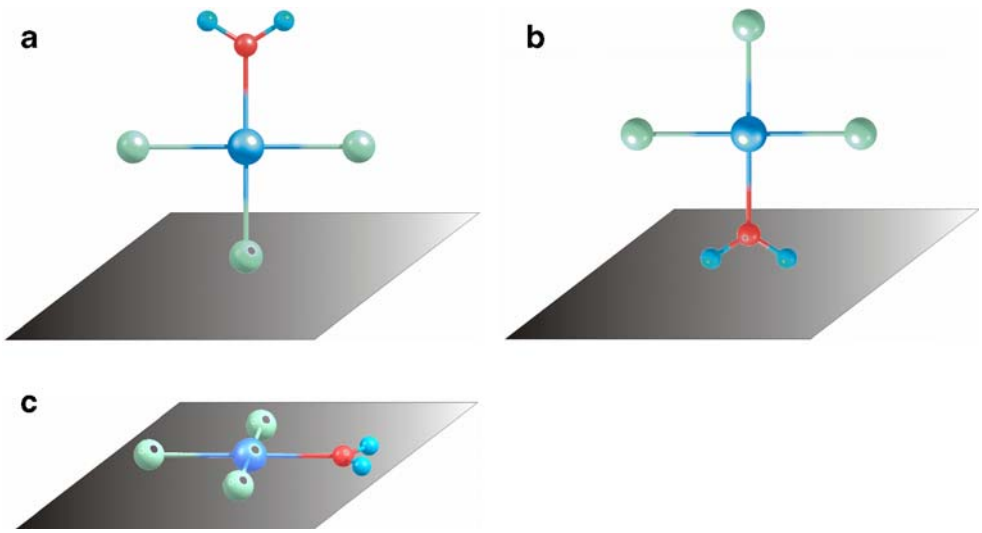

Fig. 5 Three different orientations (**a**, **b**, **c**) of $[PtCl_3(H_2O)]^-$ on the electrode surface

consider the product $k_{in}(q)P^*(q)$, which might be useful to render the results. We found that the probability distribution $P^*(q)$ can have one or two maxima; the product $k_{in}(q)P^*(q)$ demonstrates two maxima, if $-13<\lg\tau_L<-11.5$. The solvent coordinate corresponding to the main maximum of the product ($\widetilde{q}$) is interpreted as the "reaction window." The corresponding intramolecular coordinate $\widetilde{q}_{in}$ is found from the equation for the saddle line: $q^*_{saddle}(q)\big|_{q=\widetilde{q}}$. The $\widetilde{q}$ and $\widetilde{q}_{in}$ values computed for a certain interval of the solvent viscosity (at λ_{in}=0.6 eV) are summarized in Table 2. For the region of small viscosity ($\lg\tau_L=-12.2$), the ET occurs mainly in the vicinity of saddle point (q_{saddle}), while the viscosity increasing leads to a noticeable deviation of the $\widetilde{q}$ values from q_{saddle}. Then, an effective activation barrier, $\Delta E_a^*(\widetilde{q})$, is computed replacing q with $\widetilde{q}$ in Eq. 4. A measure of the reaction deviation from the saddle point can be recast as the difference:

$$\delta\Delta E_a^* = \Delta E_a^*(\widetilde{q}) - \Delta E_a^*(q_{saddle}). \quad (16)$$

As can be observed from Fig. 4, the $\delta\Delta E_a^*(\eta)$ peaks become larger when the solvent viscosity increases. The positions of peaks coincide approximately with those obtained for $\vartheta(\eta)$ (Fig. 3a). Thus, the strongest influence of solvent dynamics is observed when the avoidance of saddle point is maximal. It should be mentioned that similar calculations performed for λ_{in}=1.5 eV lead to the same conclusions. The close correlation between the model $\vartheta(\eta)$ and $\delta\Delta E_a^*(\eta)$ dependencies can be regarded as the key reason elucidating the nature of nonmonotonous viscosity effect on the ET rate.

Concluding remarks

Although in this work we considered mainly $[PtCl_3(H_2O)]^-$, the other complex form, $[PtCl_4]^{2-}$, reveals qualitatively very similar effects according to our previous estimations.[1] Note that the simulations performed above do not require any detailed knowledge about the work terms. This makes such an analysis of the viscosity effects rather attractive because the reliable calculation of the work terms is a complicated problem (Nazmutdinov et al., in preparation). The qualitative conclusions regarding the nonmonotonous viscosity influence on the ET rate (made in the previous section) seem to be of general nature and can be extended to other electrode reactions (including the bond break). The computational scheme briefly described in the "Model and computational details" section offers an efficient way to model the solvent dynamics effects for multifarious adiabatic reactions accompanied with intramolecular reorganization for a wide range of key parameters.

To gain more insight into the mechanism of electroreduction of Pt(II) aquachlorocomplexes, it would be tempting to elucidate the reactant orientation at the electrode. Three assumed orientations can be considered for $[PtCl_3(H_2O)]^-$ (see Fig. 5). It is evident that the interplay between these orientations depends on the electrode charge (overpotential). Resting on the methods developed in Nazmutdinov et al. [39], we explored the electrode-reactant orbital overlap for the orientations presented in Fig. 5. The orbital overlap (and, therefore, the electronic transmission coefficient) was found to be practically zero for the planar orientation due to the symmetry of acceptor *d*-orbital of the platinum atom. Our analysis predicts the non-zero orbital overlap for $[PtCl_3(H_2O)]^-$ positioned vertically towards the surface (Fig. 5) and the orientation *b* is even more favorable (for equal Pt–electrode distances) from this viewpoint. We believe that, in the future, considering an ensemble of different orientations for both $[PtCl_3(H_2O)]^-$ and $[PtCl_4]^{2-}$ complexes in the framework of the SM model would be helpful to clarify the nature of pit on the polarization curves observed experimentally.

The setting up of new experiments to examine the viscosity effects on interfacial ET kinetics should be aimed, first of all, at a search for qualitatively interesting features resulting from the complex interplay between the reactant electronic structure and static and dynamic solvent properties. From a theoretical viewpoint, it would be promising to combine the Agmon–Hopfild formalism with "two-dimensional" molecular dynamics simulations [40].

Acknowledgement We are indebted to Galina A. Tsirlina for many discussions and stimulating comments. Useful discussions with Alexander M. Kuznetsov, Igor G. Medvedev, and Ilya V. Pobelov are also appreciated. This work was supported in part by the Russian Foundation for Basic Research (project no. 05-03-32381a).

References

1. Sumi H, Marcus R (1986) J Chem Phys 84:4894
2. Nadler W, Marcus R (1987) J Chem Phys 86:3906
3. Berezhkovsky AM, Zitserman VYu (1990) Physica A 166:585
4. Basilevsky MV, Ryabov VM, Weinberg NN (1990) J Phys Chem 94:8734
5. Zhu J, Rasaiah JC (1992) J Chem Phys 96:1435
6. Nagasawa Y, Yartsev AP, Tominaga K, Johnson AE, Yoshihara K (1994) J Chem Phys 101:5717
7. Nagasawa Y, Yartsev AP, Tominaga K, Bisht PB, Johnson AE, Yoshihara K (1995) J Phys Chem 99:653
8. Yoshihara K, Tominaga K, Nagasawa Y (1995) Bull Chem Soc Jpn 68:696

[1] The total reorganization energy for $[PtCl_4]^{2-}$ (first electron transfer) was estimated to be smaller as compared with $[PtCl_3(H_2O)]^-$.

9. Berezhkovsky AM, Zitserman VYu, Polimeno A (1996) J Chem Phys 105:6342
10. Sumi H (1996) Chem Phys 212:9
11. Sumi H, Asano T (1997) Electrochim Acta 42:2763
12. Berezhkovsky AM, D'yakov YuA, Zitserman VYu (1998) J Chem Phys 109:4182
13. Drljaca A, Hubbard CD, Van Eldik R, Asano T, Basilevsky MV, le Noble WJ (1998) Chem Rev 98:2167
14. Okado A (1990) J Chem Phys 111:2665
15. Okado A (2000) J Chem Phys 112:8595
16. Ando K, Sumi H (2003) J Chem Phys 118:8315
17. Koper MTM (1997) J Phys Chem B 101:3168
18. Koper MTM, Voth GA (1997) Chem Phys Lett 101:3168
19. Nazmutdinov RR, Tsirlina GA, Manyurov IR, Bronshtein MD, Titova NV, Kuz'minova ZV (2006) Chem Phys 326:123
20. Bagchi B, Fleming GR, Oxtoby DW (1983) J Chem Phys 78:7375
21. Bagchi B, Fleming GR (1990) J Phys Chem 94:9
22. Fawcett WR, Foss CA Jr (1991) Electrochim Acta 36:1767
23. Weaver MJ (1992) Chem Rev 92:463
24. Fawcett WR, Opallo M (1994) Angew Chem Int Ed Engl 33:2131
25. Frumkin AN, Florianovich GN (1951) Dokl Akad Nauk SSSR 80:907
26. Kivalo P, Laitinen HA (1955) J Am Chem Soc 77:5205
27. Nikolaeva-Fedorovich NV, Petrii OA (1961) Zh Fiz Chim 25:1270
28. Kravtsov VI, Kukushkina VA (1973) Elektrokhimiya 9:1058
29. Pobelov IV, Borzenko MI, Tsirlina GA, Petrii OA (2001) Elektrokhimiya 37:270
30. Bezruchko MM, Tsventarnyi EG, Malev VV (2001) Elektrokhimiya 37:1367
31. Pobelov IV, Kuz'minova ZV, Tsirlina GA, Petrii OA (2003) Russ J Electrochem 39:828
32. Nazmutdinov RR, Pobelov IV, Tsirlina GA, Petrii OA (2000) J Electroanal Chem 491:126
33. Marcus RA (1965) J Chem Phys 43:679
34. Schmickler W (1995) Chem Phys Lett 237:152
35. Frisch MJ, Trucks GW, Schlegel HB, Scuseria GE, Robb MA, Cheeseman JR Jr, Montgomery JA, Vreven T, Kudin KN, Burant JC, Millam JM, Iyengar SS, Tomasi J, Barone V, Mennucci B, Cossi M, Scalmani G, Rega N, Petersson GA, Nakatsuji H, Hada M, Ehara M, Toyota K, Fukuda R, Hasegawa J, Ishida M, Nakajima T, Honda Y, Kitao O, Nakai H, Klene M, Li X, Knox JE, Hratchian HP, Cross JB, Adamo C, Jaramillo J, Gomperts R, Stratmann RE, Yazyev O, Austin AJ, Cammi R, Pomelli C, Ochterski JW, Ayala PY, Morokuma K, Voth GA, Salvador P, Dannenberg JJ, Zakrzewski VG, Dapprich S, Daniels AD, Strain MC, Farkas O, Malick DK, Rabuck AD, Raghavachari K, Foresman JB, Ortiz JV, Cui Q, Baboul AG, Clifford S, Cioslowski J, Stefanov BB, Liu G, Liashenko A, Piskorz P, Komaromi I, Martin RL, Fox DJ, Keith T, Al-Laham MA, Peng CY, Nanayakkara A, Challacombe M, Gill PMW, Johnson B, Chen W, Wong MW, Gonzalez C, Pople JA (2003) Gaussian 03 revision B.04. Gaussian Inc Pittsburgh PA
36. Hay PJ, Wadt WR (1985) J Chem Phys 82:270
37. Nazmutdinov RR, Tsirlina GA, Petrii OA, Kharkats YuI, Kuznetsov AM (2000) Electrochim Acta 45:3521
38. Borisevich SV, Kharkats YuI, Tsirlina GA (1999) Russ J Electrochem 35:753
39. Nazmutdinov RR, Glukhov DV, Tsirlina GA, Petrii OA (2003) Russ J Electrochem 39:97
40. Ignaczak A, Schmickler W (2002) Chem Phys 278:147
41. Ayala R, Marcos ES, Diaz-Moreno S, Solé BA, Muňoz-Páez A (2001) J Phys Chem B 105:7588